RECONSTRUCTION OF TRAJECTORIES OF TU-154M IN SMOLENSK DURING LAST SECONDS OF FLIGHT

Glenn Arthur Jørgensen

Abstract

A robust rigid body model of plane aerodynamic kinematics has been elaborated. A case study analysis has been performed with use of the model to reconstruct a vertical and horizontal trajectory of Polish Air Force one plane TU-154M during crash in Smolensk on 10.04.2010 during its last seconds of flight. The analysis revealed that the model predictions become consistent with publicly available forensic evidence upon adoption of the scenario that the plane lost a left wing tip 5.5 meters long in the neighbourhood of the claimed birch at a height of approximately 30 m above ground and about 0.6 seconds later an additional loss of left wing structure took place equivalent to about 3-5 meters wing length. The present study exposed that alleged hypothesis of a birch tree cutting-off the left wing tip of 5.5 meters long to be a key technical cause of TU-154M plane crash is inconsistent with the basic laws of physics. The independent analysis of the observed initial ground contact points of the left wing and tail of the plane crash fully confirm the plane orientation and length of the left wing as found based on the hypothesis of additional wing loss and are inconsistent with the hypothesis of a loss of 5.5m of the left wing. Results of the present work are consistent with the recorded GPS measurements and the work by Prof. W. Binienda.

Keywords *- Smolensk, Roll, Ground Trace, Tu154M, Birch Collision.*

Streszczenie

Opracowany został model aerodynamicznej kinematyki samolotu jako sztywnego ciała. Z użyciem tego modelu wykonano studium analityczne dla odtworzenia pionowej i poziomej trajektorii samolotu Polskich Sił Powietrznych Tu-154M podczas katastrofy w Smoleńsku w dniu 10.04.2010 w ostatnich sekundach jego lotu. Analiza ukazała, że modelowe przewidywania mają znaczenie publicznie dostępnego sądowego dowodu na to, że samolot stracił końcówkę lewego skrzydła o długości 5,5 m w sąsiedztwie znanej brzozy przy wysokości około 30 m nad ziemią, a następnie około 0,6 s później miała miejsce dodatkowa utrata konstrukcji lewego skrzydła równoważna około 3-5 metrów długości skrzydła. Przedstawione studium ukazuje, że domniemana hipoteza o brzozie odcinającej końcówkę lewego skrzydła o długości 5,5 m, co miałoby być techniczną przyczyną katastrofy Tu-154, jest niezgodna z podstawowymi prawami fizyki. Niezależna analiza zaobserwowanych punktów początkowego kontaktu z gruntem lewego skrzydła i ogona podczas katastrofy samolotu w pełni potwierdzają ustawienie samolotu i długość lewego skrzydła jako opartych na hipotezie dodatkowej utraty skrzydła i są niezgodne z hipotezą utraty tylko 5,5 m lewego skrzydła. Wyniki przedstawionej pracy są zgodne z zarejestrowanymi pomiarami GPS i z pracą prof.

Słowa kluczowe – *Smoleńsk, beczka samolotu, ślad na ziemi, Tu-154M, zderzenie z brzozą.*

Ms.Sc. Mech. Eng. Glenn Arthur Jørgensen (e-mail: gaj@xtern-udvikling.dk).

1. INTRODUCTION

It was the author's initial intention to justify to a colleague, that the official explanation of the crash was consistent with the basic laws of physics, aero dynamics and recorded data as by the planes "black boxes". Very soon the opposite conclusion stood clear. The problem of the official explanation is very simple*: In order for the plane to experience a roll as recorded, the rolling moment, L, must exceed a certain value* $L>L_{min}$*. As the rolling moment is driven by the difference in lift of the broken and intact wing, this again requires the loss in lift,* ΔF*, to exceed a certain value* $\Delta F>\Delta F_{min}$*.* ***The problem of the official explanation is that the plane is fare from making its way to the correct crash location given such lift loss required to explain the recorded roll, when only allowed a height of 5m at the birch tree claimed to have cut the wing, e.g. the height of the plane is significantly larger flying over the birch tree.***

Simple estimates based on dimensional analysis indicated that loss of 5,5 meter long tip of Tu-154M wing leads to loss of about 6% of lifting force. Upon such a loss of lifting force the plane should be able to safely land, and the resulting roll angle being far from the recorded roll angles. Even with the *double* loss of lifting force the calculated roll angle of the plane is significantly lower than the recorded roll angle. The loss of lifting force needs to be an estimated 16% or higher to obtain a reasonable correlation between the calculated and recorded roll angles. *It is important to note, that this can be concluded after only 1,6 sec flight following the wing loss, and the conclusion does not require an accurate calculation of the entire final 5 sec flight to crash.*

Another factor, which surprised me and aroused my engineering interest, has been the extent of the plane destruction as registered on photographic documentation from the wrecking place. Such damage can hardly be explained by a collision with a tree, an event declared in the report of the Polish State Committee for Air Accidents Investigation to be a key technical case of TU-154M plane crash – cf. [1].

In view of the above the author has undertaken an effort to develop a relatively simple model enabling prediction of flight kinematics when the plane is treated as a rigid body and to perform parametric case studies of the last seconds of TU-154M flight trajectories.

The main target of the present work is to reach conformity between modelling numerical calculations, results and experimental evidence e.g. publicly available flight trajectories registered by ATM QAR recorder. Upon reverse

engineering knowledge of the modelling assumptions leading to such an agreement of modelling and actual trajectories enable posing credible hypotheses of what happened with the TU-154M airplane during the crash in Smolensk. The main results of the present work are formulated in the abstract and last section of the paper. In section two development of the mathematical model is described together with essential assumptions, estimates and input data values. In section three case studies of flight trajectories are computed for various events scenarios supported by experimental evidence. In section four ground traces analysis has been performed.

2. RIGID BODY MODEL OF PLANE KINETICS

2.1. Mathematical model formulation of the airplanes aerodynamic behavior

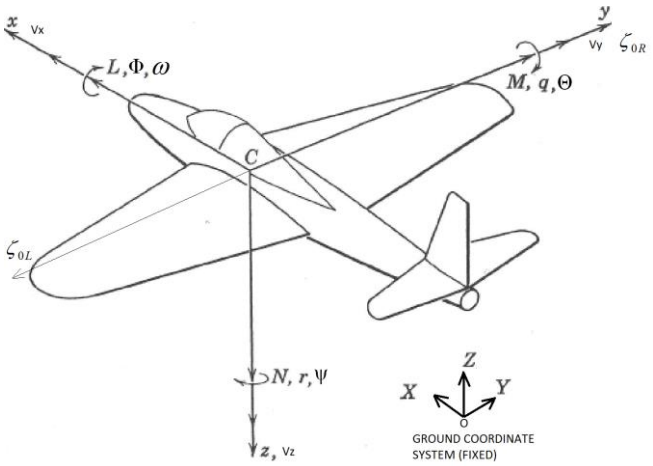

Fig. 1. Definition of the coordinate system. The figure is borrowed from [2].

The variables x, y, z represent coordinates, with origin at the center of mass of the vehicle. The x-axis lies in the symmetry plane of the plane and points toward the nose of the airplane. The z-axis also is taken to lie in the plane of symmetry, perpendicular to the x-axis, and pointing approximately down, as shown in Fig. 1. The y axis completes a right-handed orthogonal system, pointing approximately out the right wing. The variables V_x, V_y, V_z represent the instantaneous components of linear velocity in the directions of the x, y, and z axes, respectively. The variables F_x, F_y, F_z represent the components of aerodynamic force in the directions of the x, y, and z axes, respectively. The variables ω, q, r represent the instantaneous components of rotational velocity about the x, y, and z axes, respectively. The variables L, M, N represent the components of aerodynamic moments about the x, y, and z axes, respectively. The variables Φ, Θ, ψ, represent the angular rotations, relative to the equilibrium state, about the x, y, and z axes, respectively (roll angle, pitch angle and yaw angle). Thus

$$\omega = \frac{d\Phi}{dt}, \quad q = \frac{d\Theta}{dt}, \quad r = \frac{d\Psi}{dt}. \tag{1}$$

Balance of forces can be written as [2]

$$F_x = m(\dot{V}_x + qV_z - rV_y) + mg\sin(\Theta), \tag{2}$$

$$F_y = m(\dot{V}_y + rV_x - \omega V_z) - mg\cos(\Theta)\sin(\Phi), \tag{3}$$

$$F_z = m(\dot{V}_z + \omega V_y - qV_x) + mg\cos(\Theta)\cos(\Phi). \tag{4}$$

Assuming small pitch angles and small changes in pitch angle and yaw angle respectively one gets

$$\cos(\Theta) \approx 1\ ,\ \sin(\Theta) \approx 0,\ q \approx 0\ ,\ r \approx 0 \tag{5}$$

Assuming

$$qV_z << \dot{V}_x,\ rV_y << \dot{V}_x,\ rV_x << \dot{V}_y,\ \omega V_z << \dot{V}_y,$$
$$\omega V_y << \dot{V}_z,\ qV_x << \dot{V}_z \tag{6}$$

and inserting (5) into (2), (3) and (4) one gets

$$F_x \approx m\dot{V}_x \tag{7}$$

$$F_y \approx m\dot{V}_y - mg\sin(\Phi) \tag{8}$$

$$F_z \approx m(\dot{V}_z) + mg\cos(\Phi) \tag{9}$$

The balance of aerodynamic moments can be written as [2]

$$L = I_{xx}\dot{\omega} - (I_{yy} - I_{zz})qr + I_{yz}(r^2 - q^2) - I_{xz}(\omega q + \dot{r}) + I_{xy}(\omega r - \dot{q}) \tag{10}$$

$$M = I_{yy}\dot{q} - (I_{zz} - I_{xx})\omega r + I_{yz}(\omega q - \dot{r}) + I_{xz}(\omega^2 - r^2) - I_{xy}(qr + \dot{\omega}) \tag{11}$$

$$N = I_{zz}\dot{r} - (I_{xx} - I_{yy})\omega q - I_{yz}(r\omega + \dot{q}) + I_{xz}(rq - \dot{\omega}) + I_{xy}(q^2 - \omega^2) \tag{12}$$

Tab. 1. Magnitude of the various moments of inertia.

Moment of Inertia	Order of magnitude relative to $\lvert I_{xx}\rvert$	Note
$\lvert I_{xx}\rvert$, $\lvert I_{yy}\rvert$, $\lvert I_{zz}\rvert$	1	
$\lvert I_{xz}\rvert$	1/10	
$\lvert I_{xy}\rvert$, $\lvert I_{yz}\rvert$	1/100 or less	Caused by assym. wing

The equations given above are simplified by neglecting terms that are quadratic in small perturbations or products of variables of small amplitude. The moment of inertia I_{xy} and I_{yz} are zero in case of a symmetrical plane only. In the case of a wing tip loss this is of course not the case, but for the cases investigated here they still are orders of magnitude smaller than the governing moment of inertia I_{xx}, and can therefore be left out.

Thus assuming the simplified equations of motion can be written as below.

Moment about X axis

$$L = A\frac{dp}{dt} = I_{xx}\frac{d^2\Phi}{dt^2}. \tag{13}$$

From this one gets

$$\omega(t) = \frac{d\Phi}{dt} = \int \frac{L}{I_{xx}}dt \tag{14}$$

The differential equations are solved by integrating in the time domain for a simulation of the planes motion. By finding the new state as the previous state plus a change found from the previous state, the equations can be solved very simple compared to a traditional Runge-Kutta method

and an absolute rather than the relative approach, see Fig. 2. This allows basically anyone interested in verifying the calculations and results to do so without much more than a spreadsheet. Note the model can easily be expanded to include all the secondary terms quadratic in small perturbations or products of variables of small amplitude left out of this work. This is not considered important for the mission of this work and doing so should only have a minor impact on the values found, and no impact on the conclusions. This will be demonstrated in future work. On the left hand side the parameter value P(t) is found based on the state a small time distance, dt, earlier:

$$\omega_i \leftarrow \omega_{i-1} + \frac{M_{turn}(\gamma_{i-1}) - MLR\left[(-\omega)_{i-1}\right] - M_d}{-I_{xx}} \cdot dt \quad \text{E1}$$

$$\phi_i \leftarrow \phi_{i-1} + \omega_{i-1} \cdot dt \quad \text{E2}$$

$$\Delta\alpha_i \leftarrow -\text{atan}\left(\frac{\omega_{i-1} \cdot L_R}{V_{plane}}\right) \quad \text{E3}$$

$$Aw_i \leftarrow \frac{F_{wings} \cdot \left(1 + \frac{\Delta\kappa_{i-1}}{K}\right)}{M_{tot}} \quad \text{E4}$$

$$Vz_i \leftarrow Vz_{i-1} + \left(Aw_{i-1} \cdot \cos(\phi_{i-1}) - g\right) \cdot dt \quad \text{E5}$$

$$Vy_i \leftarrow Vy_{i-1} + \left(Aw_{i-1} \cdot \sin(\phi_{i-1})\right) \cdot dt \quad \text{E6}$$

$$Vx_i \leftarrow \sqrt{V_{plane}^2 - (Vy_{i-1})^2 - (Vz_{i-1})^2 + (Vz_0)^2} \quad \text{E7}$$

$$X_i \leftarrow X_{i-1} + Vx_{i-1} \cdot dt \quad \text{E8}$$

$$Y_i \leftarrow Y_{i-1} + Vy_{i-1} \cdot dt \quad \text{E9}$$

$$Z_i \leftarrow Z_{i-1} + Vz_{i-1} \cdot dt \quad \text{E10}$$

$$\Delta\kappa_i \leftarrow -\text{atan}\left[\frac{(Vz_{i-1} - Vz_0) \cdot \cos(\phi_{i-1}) + (Vy_{i-1} - Vy_0) \cdot \sin(\phi_{i-1})}{V_{plane}}\right] \quad \text{E11}$$

$$D_i \leftarrow V_{plane} \cdot i \cdot dt \quad \text{E12}$$

$$\gamma_i \leftarrow 1 + \frac{\Delta\kappa_{i-1}}{K} \quad \text{E13}$$

Fig. 2. New state values are found for the small time increment as a function of the previous state values.

Where g is the gravitational acceleration g = 9.807m/s^2 and the value K is found below. Note X, Y and Z in the above equations E1..E13 denote the position coordinates, where (X,Y,Z) = (0,0,0) at position of the wing loss. The X direction is defined as the initial plane direction prior to the loss of wing, Y direction is perpendicular to X in the span wise direction, and Z is in the direction of gravity. Aw denotes the acceleration of the planes center of gravity as a result of the wing force, and V_x, V_y, V_z the linear velocities in the X, Y and Z directions respectively.

Writing the wing lifting force, $F_{wing}(t)$, as the initial lifting force $F_0 = F_{wing}$ (t = 0) times the ratio of the overall lifting coefficient to the original lifting coefficient at t = 0, C_{z0}, one gets

$$F_{wing}(t) = F_0 \frac{C_{z0} + \Delta C_z(t)}{C_{z0}} \quad (15)$$

Assuming a linear relationship between the change in the lifting coefficient and the angle of attack, α(t), e.g. the wing is outside its stall region, one can write

$$\Delta C_z(t) = \frac{dC_z}{d\alpha}\Delta\alpha(t), \quad (16)$$

and can again be written as

$$F_{wing}(t) = F_0\left(1 + \frac{\Delta C_z(t)}{C_{z0}}\right) = F_0\left(1 + \frac{\frac{dC_z}{d\alpha}\Delta\alpha(t)}{C_{z0}}\right). \quad (17)$$

Next by defining

$$K = \frac{C_{z0}}{\frac{dC_z}{d\alpha}\alpha(t)} \quad (18)$$

equation can be written:

$$F_{wing}(t) = F_0\left(1 + \frac{\Delta\alpha(t)}{K}\right). \quad (19)$$

The corposant in the y and z directions are found as

$$F_y = F_0\left(1 + \frac{\Delta\alpha(t)}{K}\right)\sin(\Phi), \quad (20)$$

$$F_z = F_0\left(1 + \frac{\Delta\alpha(t)}{K}\right)\cos(\Phi). \quad (21)$$

The value $\frac{dC_z}{d\alpha} = 5{,}63$ can for the intact wing be found from data in [3] for the Tu-154M for a reference area of S_{ref} = 180 m^2, changing reference area to S = S_2 can be done by

$$\left(\frac{dC_z}{d\alpha}\right)_{S2} = \left(\frac{dC_z}{d\alpha}\right)_{Sref}\frac{S_{ref}}{S_2} \quad (22)$$

This value will depend on the amount of wing lost, or the remaining wing area $S_{remaining}$ as

$$\left(\frac{dC_z}{d\alpha}\right)_{S_{remaining}} = \left(\frac{dC_z}{d\alpha}\right)_{Sref}\frac{S_{ref}}{S_2}\frac{S_2 - \Delta S}{S_2}, \quad (23)$$

where the term $\frac{S_2 - \Delta S}{S_2}$ has only importance for the case of a large loss in area ΔS. (Including the term increases the estimated roll angle at the time of final recorded value by less than 1°).

The term M_d in E1 denotes a moment of resistance towards the rotation caused by air drag forces. This is estimated by regarding the wing as a number of small plates each exposed to an airflow perpendicular to the plate and with a magnitude of ω*y, where y is the local span of the plate, and integrating over both wing sides, left and right. Therefor the Cd value corresponds to the case of airflow perpendicular to a square plate (Cd = 1,15) and should not be mixed with the normal drag coefficient of a wing, which is often 10 times less. This approach merely gives a rough estimate of the moment of resistance, and is not regarded as absolute correct. Important Note: After solving the equations E1..E13, it is possible to evaluate the impact of including the term Md. It turns out, that this has neglect able influence. Including the term decreases the estimated roll angle at the time of final recorded value by less than 2°)

$$M_d := \frac{1}{2} \cdot \rho_{air} \cdot c_d \cdot \left[L_R^4 \cdot \left(\frac{B_{1R}}{5} + \frac{B_0}{20}\right) + L_L^4 \cdot \left(\frac{B_{1L}}{5} + \frac{B_0}{20}\right)\right] \cdot (\omega)^2 \quad (24)$$

where the right wing dimensions of a trapezoidal shape is

$B_{1R} := 2.138 \cdot m$ $B_0 := 7.45 \cdot m$ $L_R := 18.775 \cdot m$

and similar of the left (broken) wing

$B_{1L} := B_{lost}$ $B_0 := 7.45 \cdot m$ $L_L := L_R - L_{lost}$.

As this effect has insignificant influence it is taken out of the equations by forcing Cd = 0.

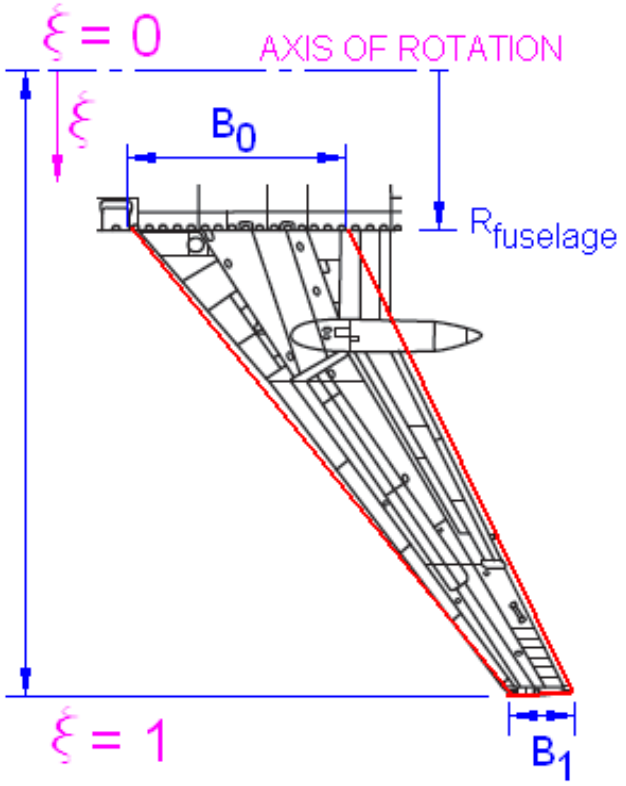

Fig. 3. Wing width and span coordinate.

B_{lost} is the width of the wing at the new wing tip, L_{lost} is the lost wing length, L_{hs} the half span length and S_{lost} the lost wing area

$$B_{lost} = \frac{B_0 - B_1}{L_{hs}} L_{lost} + B_1, \tag{25}$$

$$S_{lost} = \frac{B_0 + B_1}{2} L_{lost}. \tag{26}$$

The fuselage radius is found as $R_{fuselage}$ = 3,8/2 m = 1,9 m [3]. The parameter ζ as defined in the Fig. 3 can be found as

$$\zeta_{0R} = \frac{R_{fuselage}}{L_R}, \tag{27}$$

$$\zeta_{0L} = \frac{R_{fuselage}}{L_L}, \tag{28}$$

where B_{lost} =3,693m, A_{lost} = 16,03 m^2 , ζ_{0R} = 0,101 and ζ_{0L} = 0,143 for L_{lost} = 5,5m.

The area of a section of the wing can be written as

$$dS = [B_0(1-\zeta) + B_1\zeta]L \cdot \tag{29}$$

The moment contribution of this area, dS, can be written as the force times arm, ζL

$$dL = \zeta L_a F_a \frac{dC_z}{d\alpha} \Delta\alpha, \tag{30}$$

where the local change in angle of attack is found as

$$\Delta\alpha = a\tan\left(\frac{\omega\zeta L}{V_{plane}}\right) \tag{31}$$

The reduction in the turning moment due to the local change in the angle of attack caused by the rotation of the wing about the planes length axis (roll) can then be found as sum from both wing sides left and right. Note both wing sides left and right tend to reduce the moment, as the velocity is upwards on one side and downwards on the opposite side. For the right wing one gets

$$MR_{red}(\omega) = \int_{\zeta_{0R}}^{1} \left[a\tan\left(\frac{\omega\zeta L_R}{V_{plane}}\right)\right] \frac{dC_z}{d\alpha} L_R^2 [B_0(1-\zeta) + B_{1R}\zeta]\zeta F_a d\zeta, \tag{32}$$

and similar for the left wing

$$ML_{red}(\omega) = \int_{\zeta_{0L}}^{1} \left[a\tan\left(\frac{\omega\zeta L_L}{V_{plane}}\right)\right] \frac{dC_z}{d\alpha} L_L^2 [B_0(1-\zeta) + B_{1L}\zeta]\zeta F_a d\zeta \tag{33}$$

Adding both wings gives the total reduction of turning moment

$$MLR_{red}(\omega) = MR_{red}(\omega) + ML_{red}(\omega), \tag{34}$$

where

$$F_a = \frac{\rho_{air} V_{plane}}{2} \tag{35}$$

2.2. Adopted modeling assumption, and estimates of key parameters numerical values

2.2.1. Modeling assumptions

The model is based on the following assumptions and conditions:

1. Fixed stick control with no pilot interaction.
2. Semi-steady state conditions with balance between thrust forces/moments and drag forces/moments.
3. Terms that are quadratic in small perturbations or small variables can be neglected.
4. A linear relationship between angle of attack (AOA) and force generated by the wing surfaces is found based on the overall lifting coefficient $C_z(\alpha)$ by [4]valid for a reference area of S = 180 m^2.
5. Change of reference area to S_2 = 201,45 m^2 is done by
$$C_{z2}(\alpha) = C_z(\alpha)\frac{S}{S_2} \tag{36}$$
6. Local change in AOA can be found by the vector sum of the velocity of the existing air flow and a component caused by the wing rotation. The latter found as
$$\vec{V}_{rot}(y) = \vec{\omega} \times \vec{y} \tag{37}$$
7. The boundary conditions being the plane linear/ rotation velocity- and acceleration vectors at the location of the birch tree claimed to have cut the left wing together with the location of the initial ground contact at the site of crash as reported in [5].
8. The resulting moment driving the plane roll is found as the product of lost lifting force of the left wing, F_{loss}, based on a simple area approach and the force center distance to the planes length axis, Y_c as:
$$L = F_{loss} \times Y_c \tag{38}$$
9. The plane velocity, V_{plane}, is assumed constant. Minor changes in the plane velocity will have only little effect on the roll angles found, and no impact on the conclusions.

Loss of a wing section on one side of the plane will result in a rolling moment L, about the airplanes length axis caused by the difference in total lift of the two sides left and right. The rolling moment is found as the product of the force difference ΔF and the effective force center of this force difference (force ARM). The moment L can be found using a simple area approach assuming the total lift is equally distributed about the entire surface area of the wing, or it can be found more accurately based on sophisticated **C**omputational **F**luid **D**ynamic calculations (**CFD**) taking the actual 3D geometry and configuration of the plane into account. The first method will tend to slightly underestimate the force, and overestimate the Arm leaving the product **L= ΔF*Arm** found by both methods similar to one another. [6].

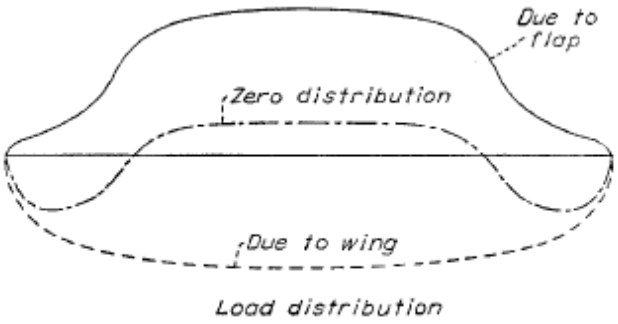

FIGURE 1.—Angle of attack and load distribution for a wing with flaps.

Fig. 4. The load distribution is dramatically changed with the use of flaps. The result is that significantly more load is carried by the inner wing sections than without the use of flaps. Here shown for the superposition of flaps distribution and normal wing distribution forming the zero distribution. Figure is taken from [7].

As the plane had slats and flaps extended in landing or go-around mode the lift distribution is changed towards significantly more lift carried by the inner sections of the wing compared to a normal cruise condition, as shown in Fig. 4. Thus the resulting moment by the simple area approach used in this work is very conservative, and only used until further work in this area is performed giving a more correct and less conservative value of the lift loss associated with a certain loss of wing length. *It should be noted, that the conclusions made in this work, are not effected by any moderate adjustments of the lost lifting force.*

2.2.2. Basic plane parameters

The plane mass M = 78,6 ton as estimated in [5]. The planes moment of inertia about its length axis (x-axis) is in the lack of data of the TU-154M estimated based on data derived from [8] for the TU-154M sister plane, the Boeing 727-200. As the Tu-154M has a maximum takeoff weight of 7% higher than the 727-200 and a 14 % larger span, this estimate is believed to be on the low (conservative) side

$$I_{xx} = 1.6 \times 10^6 \, kgm^2 . \qquad (39)$$

2.2.3. Model Solver.

The equations of the plane motion are solved in MATHCAD by a stepwise integration the equations of motion to obtain a time history of the involved main parameters.

3. VARIANT ANALYSES OF PLANE TRAJECTORIES

3.1. Case study of wing tip loss of 5.5 m occurring 5m above ground at claimed birch tree

The case investigated here corresponds to the scenario presented in the Anodina, Miller report suggesting a collision with birch tree to be the key cause of TU-154M crash in Smolensk. Fig. 5 a) shows the horizontal trajectory (red dots), the TAWS38 position (yellow dot), the final FMS position as recorded by the GPS system and the location of the birch tree (rightmost red dot). The plane is flying from left to right. The observed ground trace of the left wing is shown with a read arrow. Fig. 5 b) shows the vertical trajectory of the planes center of gravity (COG) together with the trajectory of the left wing tip (red line) and the ground height relative to the site of crash as by fig. 35 of [5] (black line). Note the left wing hereby is expected to make the ground contact about 35 m to early. As the left wing tip is only 1-2 m above ground for 100 m prior to this early point of ground contact, the left wing is expected to experience severe contact with trees and vegetation over this distance.

Fig. 5 c) shows the calculated roll angle (blue line) and some of the recorded roll angle measurements (black squares). Note the recorded roll angles are almost 100 % larger than the calculated roll angles, e.g. **the rolling moment of a wing loss of 5,5 m is insufficient to explain the encountered roll behavior**.

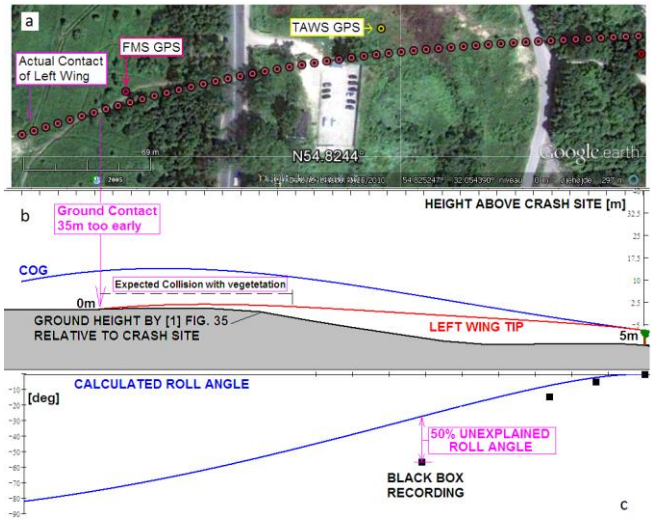

Fig. 5. Horizontal and vertical trajectories together with roll angle for the case of official wing loss. Note the left wing makes ground contact 35 m too early and 50% of the recorded roll angle is unexplained. The final roll angle is about Φ ≈ 80°, or half the value claimed in [5]. Severe collision with vegetation prior to ground contact should also be expected (not reported). The calculated horizontal trajectory ends slightly north of the crash site.

Case study of crash is **Φ ≈ -80°.** This is only about half the final roll angle of Φ = -150° to -160° reported in [5]. Note: A larger rolling moment can be obtained, if for some reason the lift loss associated with the lost wing tip is higher than estimated in this work. Of course in such case the correlation between the calculated and recorded roll angle might be slightly improved, but the distance between the calculated and recorded position of the point of initial ground contact of the left wing will as a result increase hereby worsening the difference. With other words the more lift loss the plane experiences the higher the plane needs to

be above the ground of the birch tree in order to reach the correct position of crash. A conservative estimate of the required height above the birch tree by this work is H_b = 8,5 m for a 8 % loss of lifting force, but still only half the recorded roll angle is explained, and as shown in the next chapter, the calculated ground traces for this scenario do not correlate with observations.

The results presented here deliver premises to reject the hypothesis that collision of the TU-154M with birch tree only to be a cause of crash of the Tu-154M plane.

3.2. Of wing tip loss of 9,5 m occurring 30 m above ground of the claimed birch tree

By the alternative hypothesis tested in this work the height above the birch tree is regarded as an output variable. The wing loss is identical to the official hypothesis plus an additional 3-5 m span wise loss. The recorded signal of the vertical acceleration sensor shows a second dive greater than the first (from 1,3 g to 0,2 g) about 50 m later than the first dive indicating an additional loss of lift at this time. See Fig. 6.

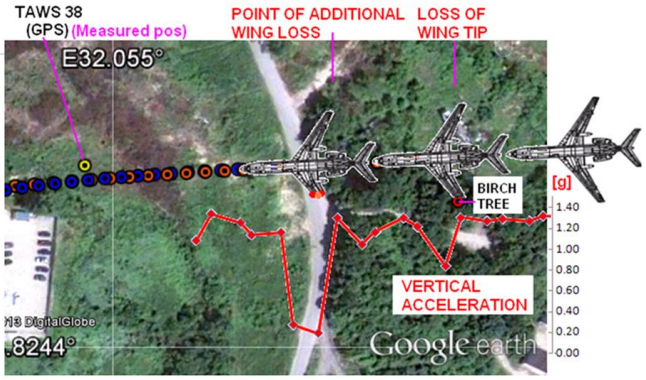

Fig. 6. The recorded vertical cceleration signal shows two distinct dives separated by about 50 m. Here the first dive is positioned over the birch tree for the purpose of illustration.

Assuming – by the authors view likely event – that the time of the second dive being the time of the additional wing loss would require an acceptance of manipulation of the timing of the recorded roll angle reported in [5]. This by moving the reported roll angle to start at the position of the second dive rather than the first or a shift of about 0,6 s. One of the goals of this work is to show the official hypothesis wrong, and there for the additional wing loss is regarded as lost together with the official wing tip loss. This allows for a good comparison of calculated roll rate towards recorded roll rate, and the need to prove any manipulation of the recorded roll angle is avoided. From an aero dynamical standpoint these two variants of the hypothesis of additional wing loss are very similar and lead to the exact same conclusions. To demonstrate the insignificant influence of the position of wing loss towards the overall conclusions another variant is calculated, where the loss takes place 30 m *prior* to the birch tree. Fig. 7 shows similar to Fig. 5 the horizontal and vertical trajectories together with the calculated and recorded roll angles for the hypothesis of additional 4 m wing loss, or a total lifting force loss of 16,5 %. Note the good correlation between the recorded and calculated roll angles.

The left wing tip in this scenario now makes contact at the correct location as reported in KBWLL (X = -518 m) [1]. The required height above the birch tree ground in this case is H_b = 30 m. which is in agreement with the recorded height by the GPS. For a loss of ΔL = 9,5 m wing tip, the estimated final roll angle at the site of crash is **Φ ≈ -135°.**

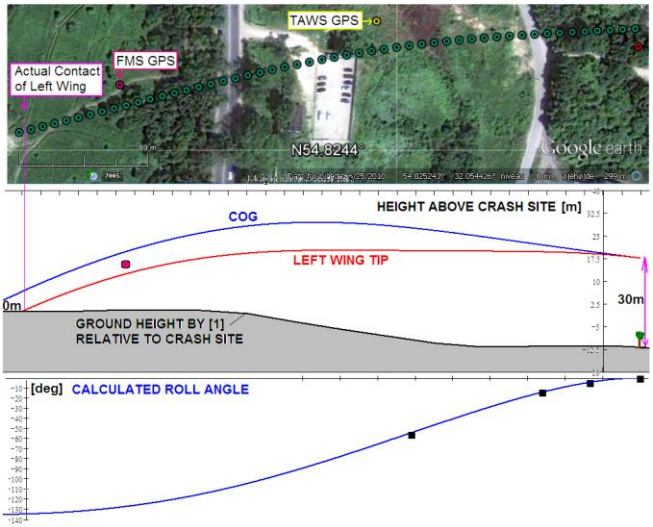

Fig. 7. Horizontal and vertical trajectories together with roll angle for the case of additional 4 m wing loss occurring over the birch tree.

In order to demonstrate the insignificant influence of the position of wing loss towards the overall conclusion another variant is shown in Fig. 8., where the loss takes place 30 m *prior* to the birch tree. In this case the height above ground at the point of loss of wing length is H_b =25 m. In this case the wing loss is slightly smaller ΔL = 8,5 m, or about 14 % lift loss. The final roll angle in this case is found as Φ = -125°.

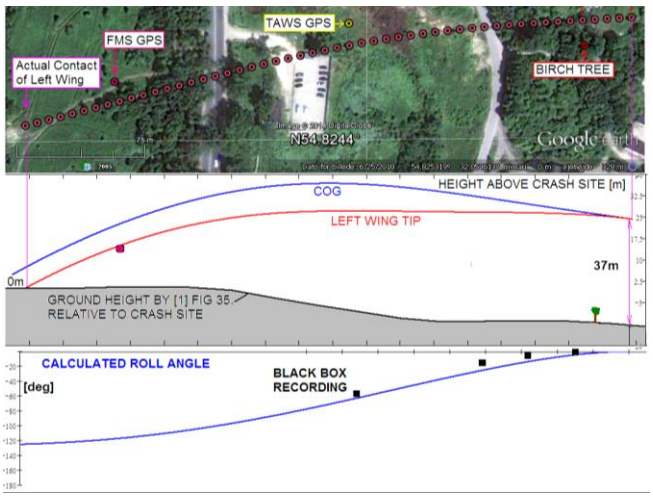

Fig. 8. Horizontal and vertical trajectories together with roll angle for the case of additional 3 m wing loss occurring 30 m *prior* to the birch tree with a lost wing length of ΔL = 8,5 m. The height of the airplane when loosing the wing section is H0 = 25 m + 12 m = 37 m above local ground. This is 7 m higher than if the wing loss occurs over the birch due to the longer distance the airplane must travel to reach the correct location of crash.

3.3. Discussion of the case studies results

Only about half the recorded roll angle and recorded angular speed of the airplane can be explained by the official hypothesis of a wing loss of ΔL = 5,5m. The calculated final roll angle, Φ ≈ -75° is only about half the reported value Φ ≈ -150° [5]. The airplane is also found to

make about 35 m too early ground contact, when assuming a height above ground at the birch tree of 5 m as claimed in [5]. The hypothesis of an additional wing loss correlates with a) the recorded roll angles, b) roll angular speed, c) point of ground contact and d) gps measurements. The final roll angle of the case of additional wing loss is found to be $\Phi \approx -135°$. The good correlation is present for the hypothesis of additional wing loss even when the point of loss is assumed 30 m prior to the birch tree, in which case the required lost wing length is slightly shorter or about ΔL = 8,5m. (Actually in several parameters this scenario correlates even better than for the wing loss occurring over the birch tree).

The aero dynamical analysis excludes the official hypothesis and strongly supports the hypothesis of additional wing loss.

4. ANALYSIS OF THE INITIAL LEFT WING AND TAIL GROUND TRACE LOCATIONS ASSUMING THE AIRPLANE MAKES GROUND CONTACT AS AN INTEGRATED STRUCTURE

4.1. Satellite experimental evidence and geometrical constraints

The satellite data taken on the 11-th of April 2010 is purchased by the author from the independent company GEOEYE and measurements are performed using Global Mapper v.14.1. See Fig. 9 and Fig. 10. The 3D model of the airplane has an outer geometry of the main parts of interest as defined in [3]. As all three motors are located at the tail, this section contains a great deal of the entire plane mass. Therefor the tail can be assumed to nearly follow the direction of the airplanes general movement prior to the wing ground contact. This allows for a prediction of the tails point of initial ground contact, given the airplanes 3D orientation and motion is known at the point of initial wing contact. The calculated point of tail contact can be compared to the observated point as found through the satelite data. This is illustrated in **Fig. 11.** where the airplane is shown for a number of different roll angles ranging from $\Phi = -137°$ to $\Phi = -100°$.

Fig. 9. Satellite photo of ground traces from 11-th of April 2010. The upper groove is the trace formed by the left wing and the lower trace the groove formed by the tail contact. The length Xwt = 15 m, of the hypotenuse of the drawn triangle is equal to the distance between the initial wing contact and initial tail contact. The short triangle leg is parallel to the plane movement prior to ground contact. The length defined as Xp = 5m.

The parameter X_{wt} is defined as the distance between the initial wing contact and initial tail contact, and is equal to the hypotenuse of the triangle drawn in Fig. 10.. The parameter X_p is equal to the distance the tail makes contact upstream or earlier than the initial left wing contact point. This distance is measured in the airplanes direction of movement projected to the ground. X_p equals the short leg of the triangle drawn in Fig. 10.. Note if the tail contact point is closer to the runway than the point of the initial wing contact, X_p will be negative. By Fig. 9. one finds X_{wt_sat} = 15 m and X_{p_sat} = 5 m.

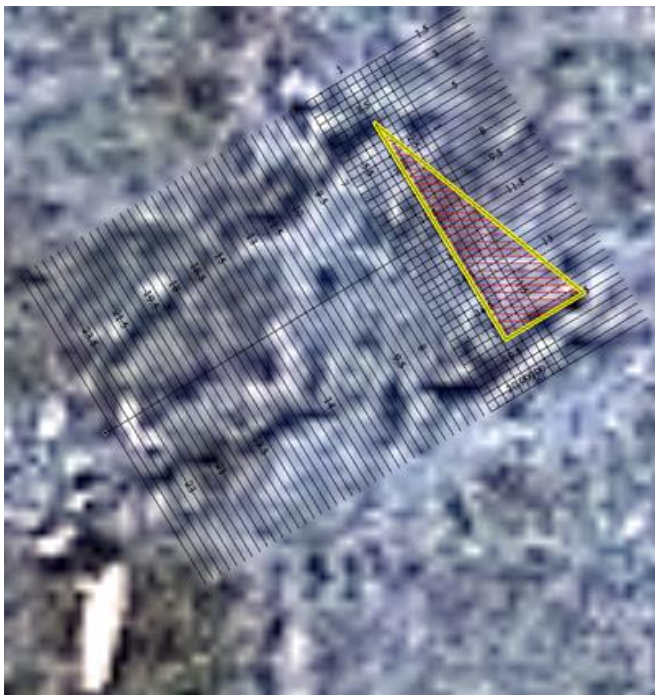

Fig. 10. Satellite photo of ground traces from 11-th of April 2010.

4.2. Case study of wing tip loss of 5.5 m

The case investigated here corresponds to the scenario presented in the Anodina, Miller reports suggesting a collision with birch tree to be the key cause of TU-154M crash in Smolensk. The final roll angle found in the previous chapter for the case of a lost wing length of ΔL = 5,5m is $\Phi \approx -75°$. As can be seen from Fig. 12 and Fig. 13 the expected tail contact point will be located far downstream (to the left) from the initial point of wing contact. This is found to be the case for roll angles up to about $\Phi = 115°$ for a wing loss of only ΔL = 5,5m.

In the figures Fig. 14 and Fig. 15 the plane is shown with a final roll angle of [5] $\Phi = -150°$. As seen the distances Xwt and Xp differ significantly from the values found by the satellite data.

The distances Xwt and Xp are plotted for different pitch angles as a function of the final roll angle of the plane, Φ. The results are shown in Fig. 16.. The best correlation is obtained for a roll angle of $\Phi \approx 139°$, but even at this rotation the distance between the tail contact with ground and the wing ground contact is at least 2 m to large.

In fact it was not possible to find a reasonable combination of roll angle and pitch angle that could result in the observed ground traces, within the orientation as found for the official hypothesis. This can be demonstrated by Fig. 16..

This delivers premises that scenario presented in Anodina, Miller reports is false.

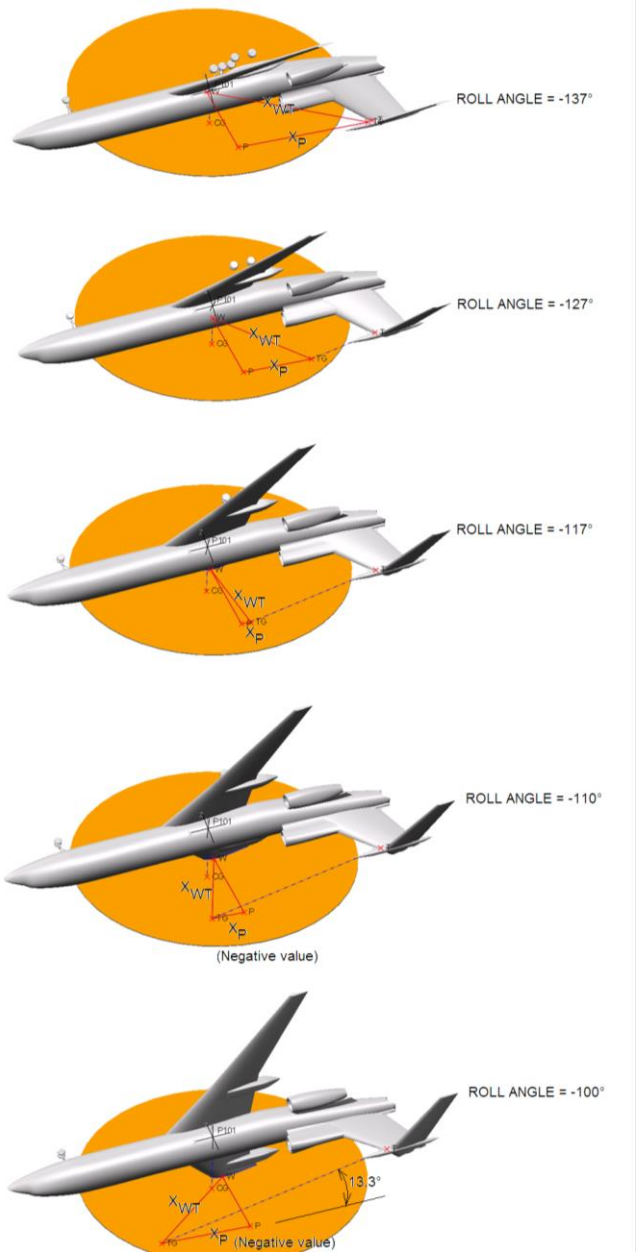

Fig. 11. The plane is shown with roll angles from -137° (top) to -100° (bottom). Note how the point of expected tail contact with ground moves from upstream (positive Xp) to downstream (negative Xp) as the roll angle decreases.

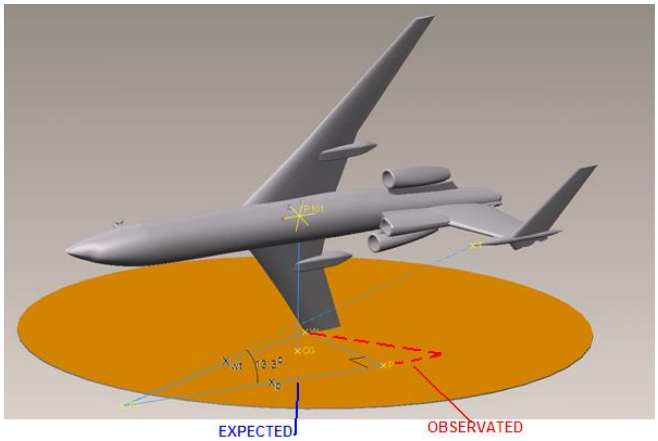

Fig. 12. The plane is shown with a roll angle of Φ = -100°. Note the tail contact with ground will be a far distance downstream compared the initial wing contact. For a roll angle of Φ = -75° this is even more severe due to the higher lift of the tail as seen in the Fig. 13.

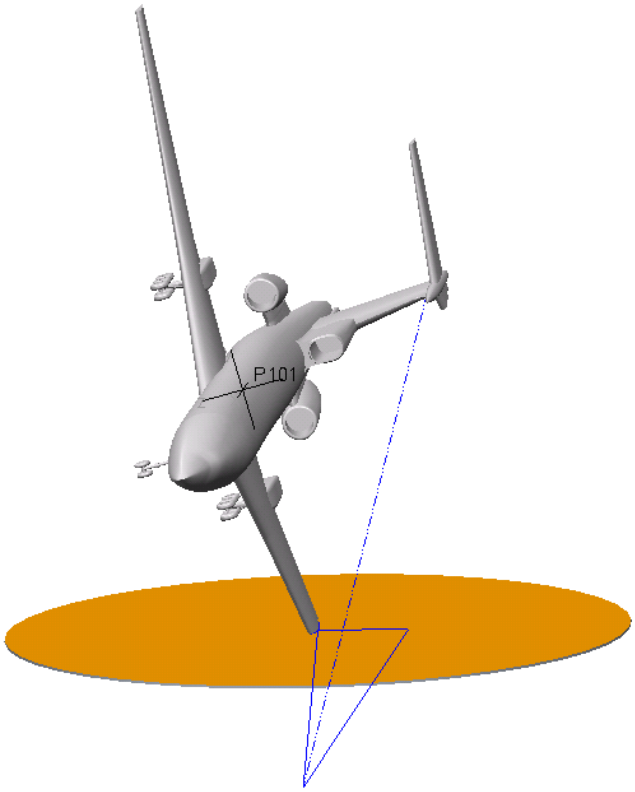

Fig. 13. The plane is shown with a roll angle of Φ = -75°. Note the tail contact with ground will be a far distance downstream compared to the initial wing contact.

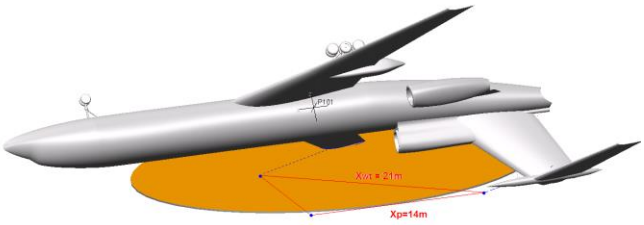

Fig. 14. The plane is shown with a roll angle of Φ = -150° as by [5]. The distance Xwt = 21 m and Xp = 14 m by no means correlate with the actual ground traces. (Side view).

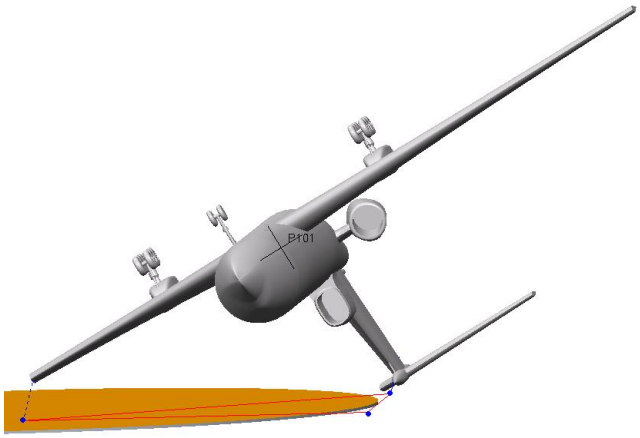

Fig. 15. Same as Fig. 14. (Front view)

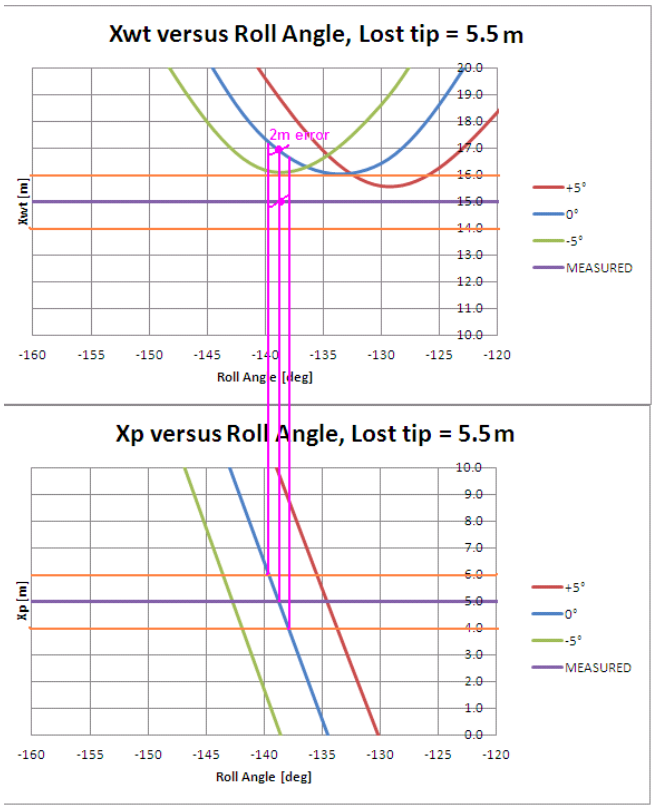

Fig. 16. The distance Xp (lower part) can be satisfied for large roll angles only, but regardless of the investigated pitch angle the distance Xwt (upper part) is 2 m to large, even when the uncertainty is set very conservative to +/-1 m for both values.

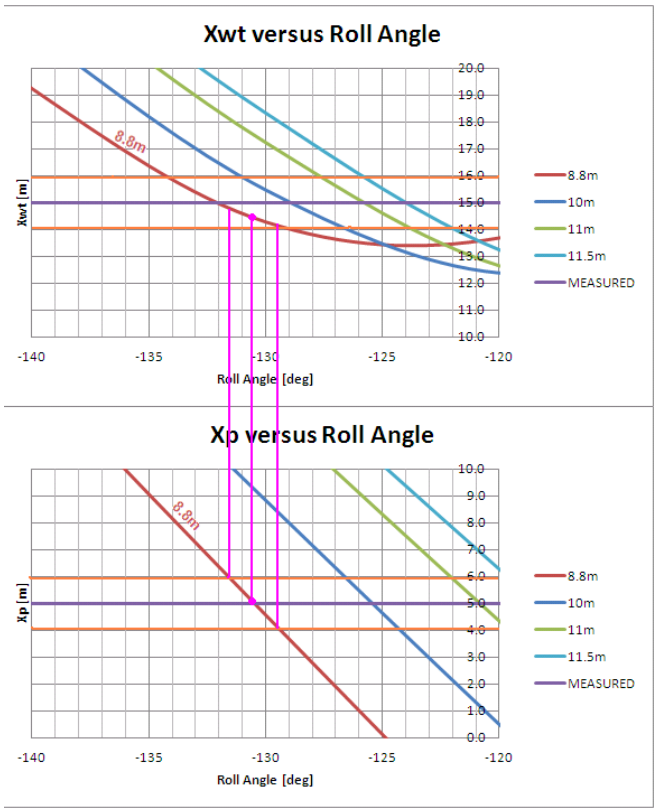

Fig. 17. The distance Xp lower part) can be satisfied for a roll angle of Φ ≈ 131° and the corresponding distance between the tail ground contact and wing ground contact Xwt = 14,5 m is very close to the value found by the satellite data, Xwt_sat = 15 m for a lost wing length of ΔL = 8,8m. The roll angle also correlates well with the value found by the aero dynamical work reported in the previous chapter.

4.3. Case study of total wing structure loss of 9 m

The combination of the shorter wing and the larger final roll angle correlates well with the observed ground traces. This can be seen from Fig. 17 and Fig. 18, where a good correlation for both of the calculated values Xwt and Xp is found for the lost wing length of about ΔL=8.8m.

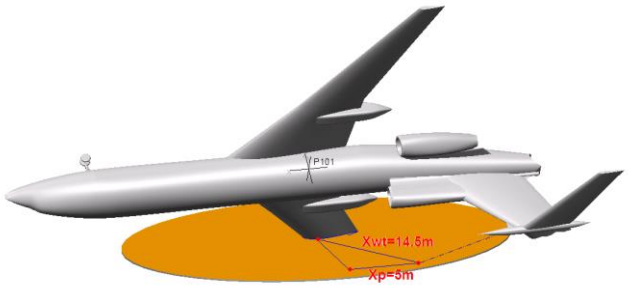

Fig. 18. The plane is shown with a roll angle of Φ = -131°, and a lost wing length of ΔL = 8,8m. Note the distance Xwt = 14,5m and the Xp = 5 m are similar to the values found by the satellite data.

4.4. Conclusions of the ground trace analysis.

The observed ground traces are incompatible with a wing loss of only ΔL = 5,5m regardless of the pitch and roll angle. The ground trace analysis suggests the planes roll angle at ground impact is in the region Φ = 130°±10°, and a lost wing length of ΔL = 8,5 m to 10,5 m.

The ground trace analysis therefore strongly supports the hypothesis of additional wing loss and excludes the official hypothesis.

5. Concluding Remarks

5.1. Current view on last seconds of flight of the TU-154M in Smoleńsk

Based on the present work including the modelled computations of the last 4-5 seconds flight of the Tu-154M as well as the analysis of the initial ground contact points of the left wing and tail and the recorded roll data, the following scenario of events most likely took place. At a location in the vicinity of the claimed birch (located N54° 49,494'; E32° 03,422' by [5]), the left wing lost first the outmost 5.5m section followed by an additional wing loss of about 3-5m about 0,5 s to 0,6 s later. To the authors view the location of the initial ground contact point of the tail and left wing suggest the plane could not have been strongly disintegrated much earlier than an estimated 0,2-0,3 s prior to ground contact, but more likely just following the wing ground contact. If the wing sections had been disintegrated much earlier than this, they would most likely have moved further away from the tail ground contact point due to the large aerodynamic forces opposed.

5.2. Summary and future work

Both the aerodynamic analysis and the ground trace analysis exclude the official hypothesis of a wing loss of ΔL = 5,5m. The lost wing length and final roll angle found by the aerodynamic analysis is very similar to the same found by the pure geometrical analysis of the ground traces.

Both methods which are completely different in nature:

1. Support the hypothesis of additional wing loss.
2. Exclude the official hypothesis.

3. *Point towards the same lost wing length $\Delta L \approx 9{,}5m \pm 1m$ and a final roll angle of about $\Phi \approx 130° \pm 10°$.*

By this the height of the airplane above the birch tree is found to be **Hb ≈ 30 m.** The hypothesis of additional wing loss is valid even if the wing loss occurs say 30 m prior to the birch, in which case the lost lengths correlate even better. The conclusions of this report agree with the work of Prof. W. Binienda [4], stating that the birch tree could not cut the wing of P101.

In future work ground traces will be further examined and the resulting moment associated with the loss of the wing section will be studied in even closer detail.

References

[1] KBWLLL report

[2] "*Introduction to Aircraft Stability and Control*" Course Notes for M&AE 5070 David A. Caughey.

[3] В. П. Бехтир, В. М. Ржевский, В. Г. Ципенко, "*ПРАКТИЧЕСКАЯ АЭРОДИНАМИКА САМОЛЕТА, Ту-154М*"

[4] "*Analysis of the Polish Govermental Plane Crash in Smolensk, Russia, on April 10, 2010*". Prof. Wieslaw K. Binienda.

[5] Interstate Aviation Committee, Air Acident Investigation Commission," *Final Report, Eng. Ver. Jan. 10th 2011*".

[6] "*Simulation of the Final seconds of Flight of P101*". Glenn A. Jørgensen. Feb 06, 2014

[7] "*Span Load Distribution for Tapered Wings with Partial-Span Flaps*". 1937, Pearson, H. A.

[8] Fig. 3.1 from Airplane Design, Part V:"*Component Weight Estimation*", by Dr. Jan Roskam, 2003.